J Nondestruct Eval (2015) 34:1
DOI 10.1007/s10921-014-0275-3

Ultrasonic Evaluation of Residual Hoop Stress in Forged and Cast Railroads Wheels—Differences

Jacek Szelążek

Received: 8 September 2014 / Accepted: 18 December 2014 / Published online: 6 January 2015

Abstract Paper describes the assessment of hoop residual stresses in the rim of monoblock railroad wheels using ultrasonic methods. Dangerous tensile stress builds up during service as a result of heat loads caused by braking with braking blocks/brake shoes. Results of experiments on two types of monoblock wheels are described: on rolled-forged wheels used in Europe and on cast wheels manufactured and used in North America. Stresses in forged wheels are evaluated with birefringence technique. Investigations carried out in various countries, using different ultrasonic equipment, proved that an ultrasonic technique can provide valuable information concerning stress values in wheels during manufacturing and in service. However, they also showed that due to different microstructures in the rim material and differences in wheel plate design, forged and cast wheels present unique problems for ultrasonic stress evaluation. The aim of this paper is to emphasize these differences and to illustrate how they influence ultrasonic readings. The second ultrasonic technique to evaluate stress is proposed to standard cast wheels – technique based on measurements of time of flight of subsurface (surface-skimming) longitudinal waves propagating in hoop direction on both rim faces. Presented data are based on detailed measurements of acoustic properties of monoblock wheel materials and on earlier experiments performed on forged and cast wheels subjected to inductive heating, braking in a test stand or on track.

Keywords Ultrasonics · Acoustoelasticity · Residual stress · Railroad wheels

J. Szelążek (✉)
Institute of Fundamental Technological Research, Pawińskiego 5B, 02-106 Warsaw, Poland
e-mail: jszela@ippt.gov.pl

1 Introduction

As-manufactured monoblock railroad wheels are subjected to heat treatment resulting in a compressive residual hoop stress in the rim. During braking with braking blocks/shoes, friction causes wheel rim temperatures to be higher than the temperatures of wheel plates and hubs. Thermal expansion of the material creates a compressive hoop stress in the rim and tensile hoop stress in the wheel plate. If the thermal hoop stress is higher than the elastic limit of the hot and plastic wheel material, plastic deformation occurs. After braking, during wheel cool down, the deformed rim contracts and a tensile hoop stress is created in the rim. Repeated high power braking applications can cause a build-up of this hoop stress, which can contribute to crack growth in the rim. In the railroad community, wheels with high tensile stress are called "explosive" because they can catastrophically shatter without any warning during cool down. In the 1980s, the development of stresses in the wheel rim was theoretically modeled and destructively evaluated [1,2]. A simple destructive method used to evaluate hoop stress was radial cutting of the wheel from tread to hub. Closure of the cut indicated compressive stress; opening of the cut indicated a tensile stress condition. In the US, it was often observed in cast, curved plate wheels that the slot on the back rim face (BRF) opened but closed on the front rim face (FRF) what indicated significant hoop stress gradient in the rim [3].

Numerous nondestructive methods were also tested. A magnetoacoustic technique was investigated in the US [4], magnetic techniques were tested in Australia [5], an X-ray diffraction technique was applied in Japan [6] and Barkhausen noise was used in the US [7]. After years of experiments, an ultrasonic technique based on acoustic birefringence measurement, was chosen as the most promising one. It was shown to be reliable, able to be applied in

industrial conditions such as in workshops or on track, and quickly able to evaluate stresses in wheels of various designs, of various steel grades. The advantage of this technique was that it delivers information about stress value averaged over the rim width.

The history of ultrasonic stress evaluation in monoblock wheels is more than 40 years old. The first paper describing ultrasonic stress evaluation in the cast wheels was published in 1968 in the US [8]. The author achieved promising results measuring acoustic birefringence in the wheel rim. However, the technique was not then ready to be used in industrial conditions. In 1984, cast and forged wheels were ultrasonically measured [9] with the same technique. In 1986, acoustic birefringence was evaluated for the first time using electromagneto-acoustic transducers (EMAT) [10]. The results described in this paper were limited however to only one wheel. More extensive measurements on cast wheels with EMAT transducer were published the next year [11]. In 1989, the International Union of Railways presented a report describing nondestructive and destructive investigations of stress development in forged wheels braked on test stand and in service [12,13]. Hoop stress was evaluated with the ultrasonic technique using piezoelectric transducers and with X-ray diffraction. During ultrasonic measurements, two techniques were used: one based on acoustic birefringence and the second one—on time of flight (TOF) of subsurface (surface-skimming) longitudinal waves propagating in hoop direction along the rim faces. The latter provides hoop stress values in the surface layer of rim face. Thickness of this layer is comparable to the wavelength.

The same time in Germany stresses and texture in monoblock wheels were studied with EMAT transducers designed to evaluate acoustic birefringence in the wheel rim [14].

In 1995, the first data collected in Europe on numerous monoblock wheels in service was presented, performed using various ultrasonic devices [15]. The same year, results of ultrasonic stress evaluation on both cast and forged wheels subjected to braking in test stands were published [16]. For the first time it was experimentally observed that hoop stress distribution in European (rolled-forged) and American (cast) wheels differ mostly due to different plate shapes (which confirmed earlier observations presented in [3]). It was also noted that the ultrasonic technique based on acoustic birefringence is suitable for assessment of the stress state in European wheels having a symmetric positioning of the rim in relation to hub and uniform hoop stress distribution along the rim width, while supplying less information for non-symmetrical American curved-plate cast wheels. In 1998, a summary of ultrasonic stress evaluation in cast wheels subjected to inductive heating and braked in a dynamometer was published [17]. These extensive experiments were performed with both types of ultrasonic transducers (piezoelectric and EMAT) and with two ultrasonic techniques (based on acoustic birefringence and subsurface waves).

Meanwhile, various ultrasonic devices were designed and built, mainly for acoustic birefringence measurement able to determine rim width averaged (RWA) hoop stress: the Debro [18] and Debbie [19] devices equipped with piezoelectric transducers, several devices equipped with EMAT transducers, such as the German UER device [20], an American device [21] and a French instrument [22]. German UER device was equipped with special, mechanized probe enabling automatic measurement of birefringence distribution in the radial direction. The Debro device, equipped with various probeheads, was able to evaluate both RWA stress and surface stresses on the FRF and BRF.

Today in Europe, ultrasonic stress evaluation in forged wheels is mandatory and is an everyday routine. Accepted and described in the Standard [23] method is based on acoustic birefringence measurement. Residual hoop stress measurements are not required on American cast wheels, either new, or in service [24]. It is explained that American cast wheels with "low stress" plate shape resist thermal stresses from braking in service.

Cast wheels enter European railroads. Hoop stress will be evaluated in these wheels probably with established ultrasonic technique, based on acoustic birefringence measurement. Numerous experiments showed however that due to different wheel design and rim structure, cast wheels are more difficult to be evaluated with this technique. This paper compares the results of ultrasonic investigations on forged-rolled and on cast wheels and proposes a new technique of hoop stress evaluation in curved-plate cast wheels.

2 Acoustic Birefringence Measurement

Hoop stress evaluation in monoblock wheels based on acoustic birefringence measurement was accepted by some European railroading regulatory organizations because is easy to use, delivers rim width averaged hoop stress value, measurements can be performed with access to only one side of the wheel, on new wheels in the steel mill, on used wheels in workshop or on track. Both piezoelectric and EMAT transducers can be used to launch and detect the shear waves required to make measurements. From an important, practical point of view, the advantage of this technique is that results of measurements are not dependent on rim temperature or temperature gradients along the ultrasonic wave path.

Acoustic birefringence is a measure of the relative velocity difference between two orthogonally polarize shear waves propagating along the same path. In the wheel rim, it can be measured with the pulse-echo method between two flat and parallel rim faces. The probehead for shear SH waves is coupled to the flat FRF or BRF, as shown in Fig. 1.

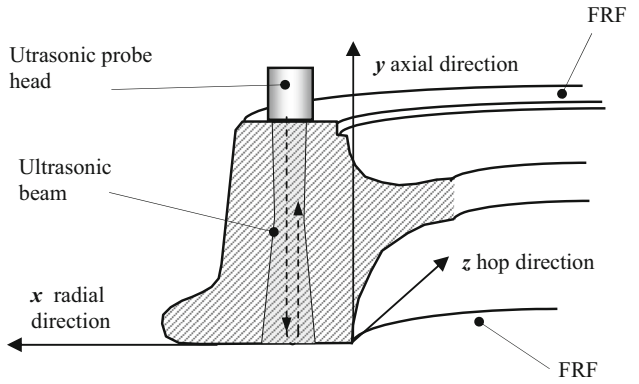

Fig. 1 Schema of acoustic birefringence measurement in a monoblock wheel rim

Measured values are TOFs of shear waves propagating in the y direction and polarized in the hoop (z) and radial (x) directions. It is assumed that wave polarization directions coincide with material acoustic axes. This assumption can be made for rolled wheels because the material texture axis and the dominant residual stress component coincide with hoop and radial directions. In the case of cast wheels, some mismatch of texture and stress directions was observed in the vicinity of casting risers as described below.

The value of acoustic birefringence B in the rim is calculated as:

$$B = B^0 + B^\sigma = \frac{2(t_X - t_Z)}{t_Z} \tag{1}$$

where:

- B^0 birefringence due to material texture,
- B^σ birefringence due to hoop and radial stresses,
- t_Z TOF of the wave polarized in hoop direction,
- t_X TOF of the wave polarized in radial direction.

B^0 has to be determine experimentally on stress-relieved rim blocks and can be expressed in units of dimensionless birefringence or in stress (MPa).

Anisotropy caused by stresses (B^σ) in the rim is:

$$B^\sigma = \beta_B\,(\sigma_Z - \sigma_X) - B^0 \approx \beta_B\,\sigma_Z - B^0 \tag{2}$$

where:

- σ_Z hoop stress component,
- σ_X radial stress component,
- σ_B "birefringence" elastoacoustic constant equal to $\beta_{122} - \beta_{132}$.
- $\sigma_{j,j,k}$ elastoacoustic constant: i, j, k denotes direction of propagation, polarization and stress respectively.

The axial stress component σ_X doesn't influence the birefringence value, since TOF changes for both waves due to this stress component are similar. The value of σ_X on the tread is zero. It can be assumed that the value of σ_X in the vicinity of the tread is small compared to σ_Z and can be neglected.

Elastoacoustic constants β_{122} and β_{132} are determined experimentally during tensile test of the sample made of the same steel grade as wheel material and calculated as:

$$\beta_{ijk} = \frac{t_0 - t_\sigma}{t_\sigma\,\sigma} \tag{3}$$

where:

- β_{ijk} elastoacoustic constant for shear wave, indexes i, j, k denote direction of propagation, polarization and stress respectively,
- t_0, t_σ TOFs in stress free and stresses condition respectively,
- σ stress.

To evaluate hoop stress in the rim, it is necessary to know experimentally determined values of B^0, β_B and to measure the TOFs t_Z and t_X in the wheel rim.

An evaluation of birefringence-based hoop stress provides information averaged over the material volume in a cylindrical shape with a diameter approximately equal to the transducer size (usually 10–15 mm) and a length equal to the rim width (about 140 mm). Figure 1 presents the approximate shape of the ultrasonic beam generated by a 12 mm, 2 MHz transducer. Averaging gives useful information about stress state—stress value proportional to the hoop net force in the rim. But averaging can be a disadvantage when applied to wheels having a high stress gradient over the rim width (in y direction).

With the birefringence technique, taking readings at various radial positions of the transducer, one can determine the radial distribution of first B^0 and then B^σ, assuming the rim face is flat and wide, and the transducer is small enough for such experiments. Such measurements are performed on new wheels which, according to Standard [23] should present specified radial stress distribution.

2.1 Elastoacoustic Coefficient

Value of the elastoacoustic coefficient has to be measured experimentally during tensile tests on samples made of the same material and texture as the wheel to be examined. Usually, samples are cut from the wheel rim, in the hoop direction. Shape of the rim limits their size and sample cross section is usually much smaller compared to the wheel rim. In result TOFs are measured on short distances determined by sample thickness. This, along with slight velocity changes

due to stress, are probably the reason why values of β_B in the literature show significant scatter. For forged wheel made of R7 steel grade, values of $\beta_{122} = -0.57 \times 10^{-5}$, $\beta_{132} = 0.22 \times 10^{-5}$ MPa^{-1} (see Eq. 3) were measured and $\beta_B = -0.79 \times 10^{-5}$ MPa^{-1} was calculated [12]. The same value of elastoacoustic coefficient was measured in [25]. In [26] the elastoacoustic coefficient β_B measured on samples cut from various forged wheels and various manufacturers, ranged from $\beta_B = -0.93 \times 10^{-5}$ up to -1.06×10^{-5} MPa^{-1}. The authors decided to use $\beta_B = -0.95 \times 10^{-5}$ MPa^{-1} for their stress calculation. In [27] the value of $\beta_B = -0.73 \times 10^{-5}$ was reported and in [28] value of $\beta_B = -0.81 \times 10^{-5}$. The recent data concerning elastoacoustic coefficient for rolled-forged wheels were presented in [29]. Authors tested samples cut in hoop and in radial directions of steel grades 2 and ER7 wheels. Measured value of elastoacoustic coefficient was $\beta_B = -0.74 \times 10^{-5}$ MPa^{-1}. Measurements showed that variations in elastoacoustic coefficient for samples cut in various directions regarding hoop and radial direction, and cut from various locations in the rim, are below 5 %.

The majority of authors determining elastoacoustic coefficient β_B for forged monoblock wheels made of typical steel grades agree that value of this coefficient is in the range $\beta_{\mathrm{BMIN}} = -0.74 \times 10^{-5}$ MPa^{-1} and $\beta_{\mathrm{BMAX}} = -0.9 \times 10^{-5}$ MPa^{-1}.

Less data regarding elastoacoustic coefficient are available for cast wheels. Initially, the value of the this coefficient for a cast steel sample, presented in 1980 [30], was determined to be -0.76×10^{-5}. In [31] presented were values of β_B measured on samples cut from cast wheels and subjected to compression and tension. The wheels were manufactured in two different manufacturing plants. For both samples, the linear dependence of TOF-stress were observed, but β_B values showed significant differences and were equal to -0.78×10^{-5} and -0.95×10^{-5} depending on the manufacturer. In measurements described in [32] a value of $\beta_B = -0.78 \times 10^{-5}$ was used to calculate stress value. In [25] values from -0.76×10^{-5} up to -0.91×10^{-5} were measured on various cast wheels. The difference between values measured on cast wheel samples from various manufacturers was shown to be as large as 20 %.

2.2 Texture-Induced Anisotropy

After rolling wheel rim material exhibit texture (preferred grain orientation) and is anisotropic. The directions of the acoustic axis of the rim material, determined by material texture, are aligned with hoop and radial directions. The value of texture induced anisotropy B^0 can be determined experimentally on rim blocks cut from a given wheel type and subjected to stress relieving heat treatment. Researchers agree that in contemporary forged wheels made of continuous cast steel, B^0 is small, evenly distributed over the wheel circumference and, in practice, the influence of B^0 on stress readings can be neglected [33,34].

Results of extensive measurements performed on numerous wheels subjected to various braking conditions, in trains moving along usual track, were published in 1998 [34]. Detailed measurements performed with EMAT transducer automatically measuring birefringence value every 1 mm step in radial direction, on more than 100 wheels, showed that for modern steel grade (R7) the influence of material texture on stress reading is small, equivalent to stress value scatter less than ±20 MPa only.

It is worth to notice that the birefringence technique is sensitive not only to texture and hoop stress, but also to even small impurities in the material. During the rolling of hot steel, impurities are elongated in the hoop direction and become an additional source of acoustic anisotropy (impurity-induced acoustic anisotropy) and can dramatically change the B^0 value. It was observed during measurements on certain old forged wheels made of ingot steel that clusters of elongated inclusions, small enough not to be detected during standard ultrasonic testing, can locally change B_0 resulting in stress evaluation error up to 500 MPa. The author observed regions on such wheels that were about 50 mm long in the hoop direction and surrounded by material regions free of impurities. In the case of localized regions of very high acoustic birefringence indications, impurities can be assigned as a source of false readings.

Figure 2 presents a summary of B^0 measurements during almost 40 years on stress-relieved rim blocks cut from forged wheels made of various steel grades, of various designs and produced by various manufacturers (A. Brokowski, private communication). One can notice that scatter of B^0 value is proportional to its absolute value. It should be emphasized that the data shown in Fig. 2 were collected on limited number

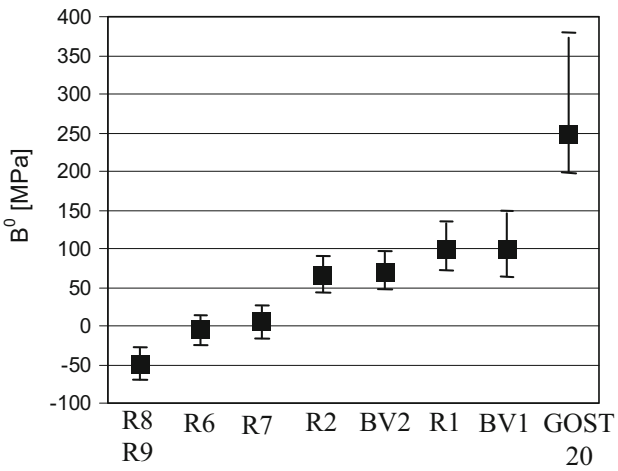

Fig. 2 Dependence of B^0 on steel grade

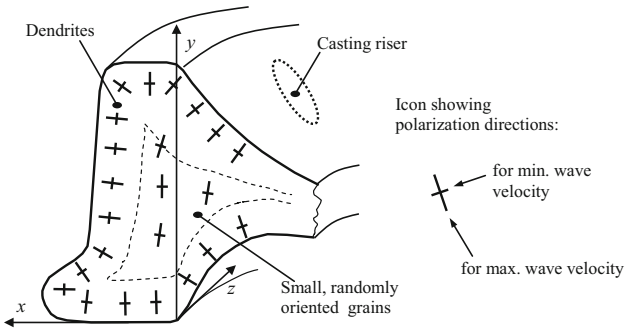

Fig. 3 Cross section of cast wheel rim. *Crosses* show directions of acoustic axis measured on the rim slice with shear wave propagating in z direction

of rim blocks and presents B^0 scatter rather than its exact value.

In modern forged, impurity-free wheels, B^0 is constant over the wheel circumference. For example in [25] described are results of B^0 measurements on three forged wheels showing scatter lower than ± 3 MPa. Readings taken on several as manufactured wheels made of R7 steel grade and described in [12] showed scatter of ± 10 MPa only.

In contrast to forged wheels, the cross section of a cast wheel, shown in Fig. 3, presents a typical heterogeneous cast structure—columnar grains on the boundaries and small, randomly oriented grains in the central part of the rim (shown by a dashed line). The outer regions are composed of a few millimeters long dendrites oriented perpendicular to the rim surfaces. Cross-like icons on the rim cross section represent directions of an acoustic axis determined on a slice cut from a cast wheel, with shear waves propagating in the z direction. The longer portion of the icon shows the direction of wave polarization for maximum wave velocity; the short portion shows minimum velocity. It can be seen that when evaluating hoop stress using shear waves propagating in the y direction, the waves cross regions with an acoustic axis not exactly parallel or perpendicular to the wave propagation direction.

Another feature of cast wheels that can influence B^0 value is a circumferential distribution of material texture caused by several casting risers located on the wheel plate, as shown in Figs. 3 and 4. Casting risers, evenly distributed on the wheel circumference, are a source of a nonsymmetrical temperature gradients during material solidification and cooling and can change directions of dendrites locally. It was observed that in as-manufactured cast wheels in the vicinity of casting riser, the direction of acoustic axes determined with shear wave propagating in y direction do not exactly coincide with the hoop and radial directions. Figure 4 presents the results of shear wave TOF measurements taken with the probehead coupled to the rim face about 50 mm from the casting riser. For probehead locations farther away from the riser and close to the tread, the acoustic axes match radial

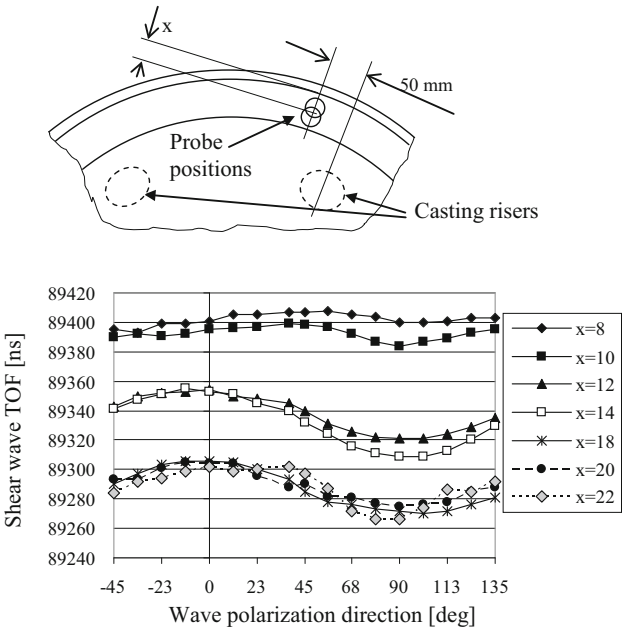

Fig. 4 TOF of shear wave propagating close to the casting riser measured for various polarization directions and radial probe head positions

and hoop directions. But for measurements taken with the probehead close to the inner rim edge and close to a riser (x = 20 and 22 mm), the acoustic axes are rotated. Due to casting risers, variations of B^0 value along the wheel circumference can lead to stress estimation error up to 50 MPa. Fluctuations of acoustic axis directions were not observed for readings taken between casting risers.

Differences in TOF due to proximity of a casting riser are small, but non-symmetrical acoustic properties of the cast rim can be a source of different readings between and near the risers. An example of such reading variation probably due to a local influence of casting risers on B^0 is presented in Fig. 5. The diagram shows acoustic birefringence values

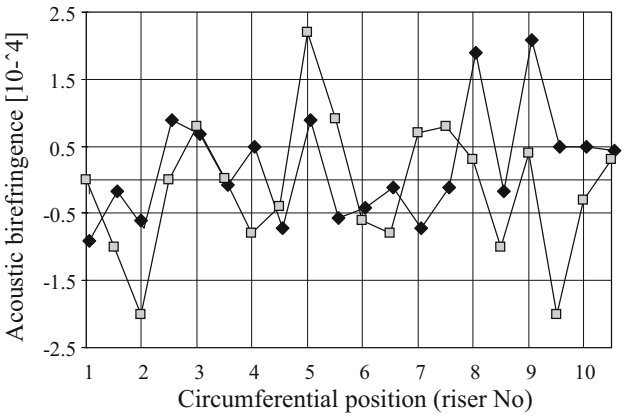

Fig. 5 Circumferential distribution of acoustic birefringence in two as-manufactured cast wheels

measured close to the casting risers and also between them in two as manufactured cast wheels. Measurements were taken with a piezoelectric probehead coupled to the FRF [32]. Significant differences between measurements taken on and between risers can be seen. Of interest, readings on some risers present a higher value of birefringence while lower on others. Assuming a constant value of compressive hoop stress over the circumference in an as-manufactured wheel, the source of certain scatter could be casting risers and their influence on B^0 value. The scatter of acoustic birefringence in as manufactured wheels, presented in Fig. 5, is equivalent to the stress variation ±60 MPa. The same circumferential distributions of readings were observed for both piezoelectric and EMAT transducers [32]. On some cast wheels, the positions of casting risers can be seen on the wheel plate. In such cases, to avoid casting riser influence on acoustic birefringence measurements, ultrasonic readings can be taken between risers. On others, to increase fatigue strength, the plate is ground smooth and risers cannot, unfortunately, be seen.

Both the complex structure of a cast wheel rim and casting risers result in a much higher scatter of B^0 value compared to forged wheels. For example, in [35] presented are the result of B^0measurements on cast wheel rim blocks from four production plants. For the same radial position of the probehead, $B^0 = -7.5 \pm 6.5 \times 10^{-4}$ (–) meaning that according to formula (2), stress can be calculated with an accuracy of ±80 MPa only. Similar high scatter of B^0values was presented in [25]. Values of texture induced anisotropy for various cast wheels, measured on stress relieved samples, were reported from $B^0 = -6.8 \times 10^{-4}$up to $+16.7 \times 10^{-4}$what is equivalent to stresses from 74 up to −190 MPa.

For both cast and forged wheels, values of B^0 depend on radial position of the probehead. Examples of radial distribution of B^0 in forged wheels measured with the probehead coupled to the FRF are presented in Fig. 6. Radial position of the probehead was measured from the front rim inner edge and for each wheel measurements were performed for two positions of the probehead on the wheel circumference. It can be seen that radial distributions of B^0 vary from wheel to wheel, but for each forged wheel type, its distribution is constant on the wheel circumference and B^0 radial variations equivalents are limited to about ±20 MPa for each wheel type.

In cast wheels, various radial distributions of B^0 were observed. As shown in Fig. 7, depending on rim thickness (single wear or multiple wear wheels) and probehead position, ultrasonic waves cross regions built of small grains and dendrites. Close to the rim faces, they propagate along the axis of the dendrites. Velocities of shear waves propagating in the y direction in this columnar region were measured on a small rectangular sample cut from a cast wheel in the region of dendrites on the BRF. As expected, no dependence of velocity-polarization was observed, meaning that B^0 in regions close to front and back rim faces is zero [36]. In an inner part of the rim,

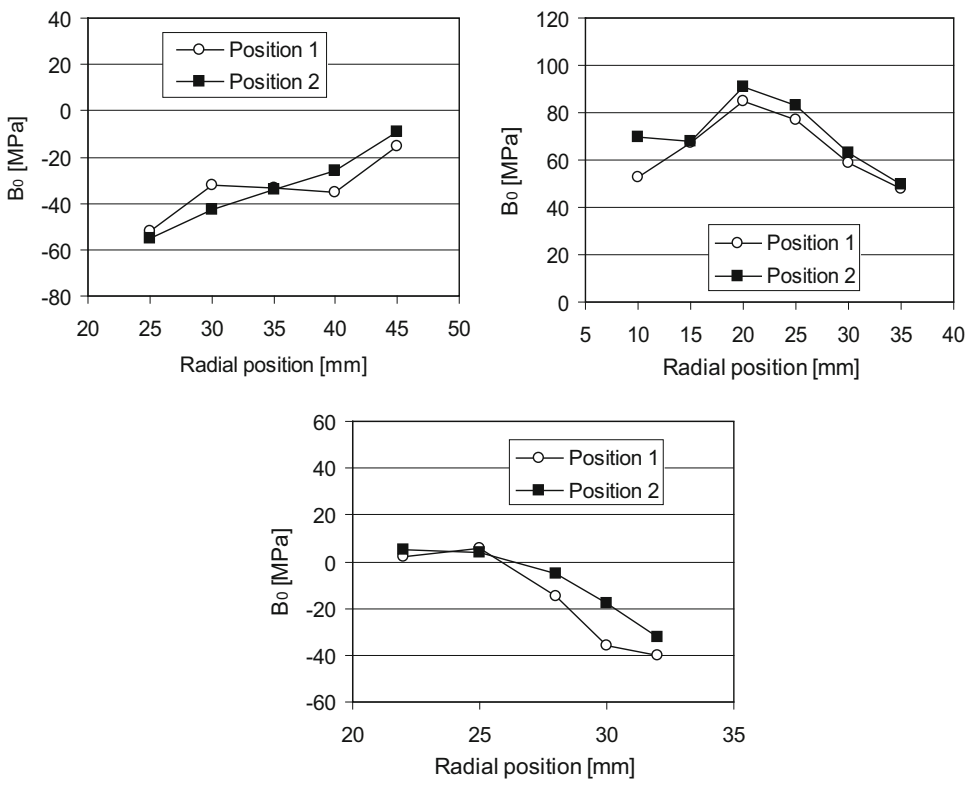

Fig. 6 Examples of radial distribution of B^0 in various forged wheels

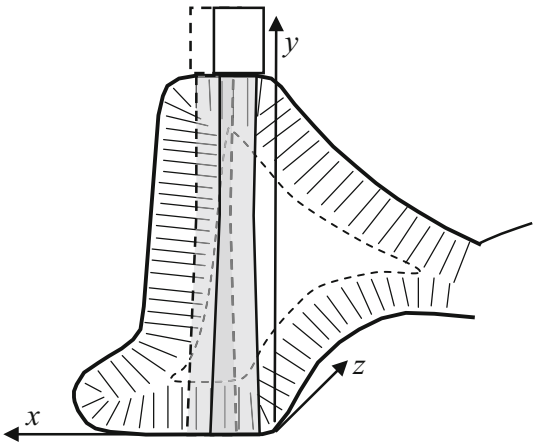

Fig. 7 Ultrasonic beam propagating in cast wheel for two probe head positions

the waves partly propagate in a region of small grains, and partly cross dendrites oriented almost perpendicular to the propagation direction. In the dendritic region, the difference between velocities of shear waves polarized in the x and z directions is equal to 10 m/s [36]. The acoustic birefringence for such velocities difference (formula 1) is equal to -3.09×10^4 (–) or equivalent to about 40 MPa. The main reason why B^0 in cast wheels reaches higher values is probably propagation of the shear waves across regions presenting various values of velocity and wave attenuation coefficient. Figure 8 presents two extreme examples of the radial distribution of B^0 in cast wheels measured with a 2 MHz, 12 mm piezoelectric transducer [32]. The first example shows nearly uniform and very low B^0 values, the second one shows a strong radial dependence of B^0.

The examples presented in Figs. 6 and 8 show that to precisely evaluate radial distribution of hoop stress with the birefringence technique, it is necessary to know radial distribution of B^0value for a given wheel type. Neglecting it and using a mean value of B^0 to evaluate radial stress distribution leads to an error reaching ±20 MPa in the case of forged wheels and ±60 MPa in the case of cast wheels.

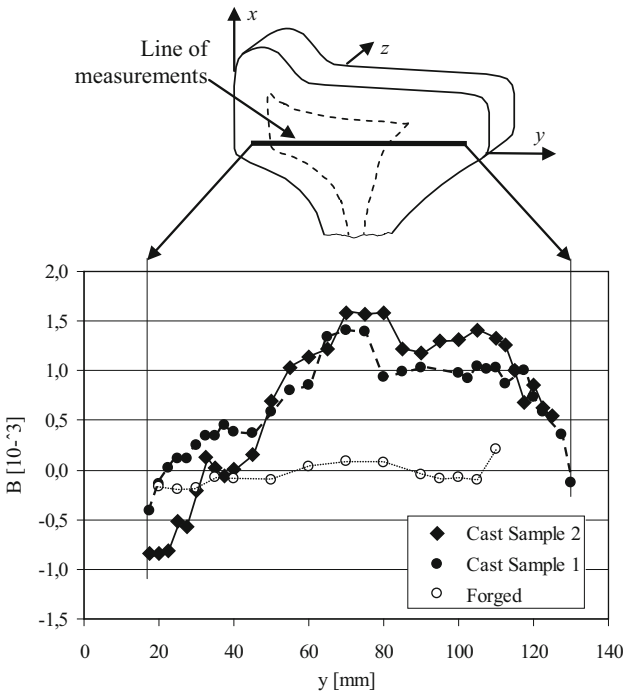

Fig. 9 Acoustic birefringence measured on slices cut from cast and forged wheels measured with shear waves propagating in z direction and polarized in x and y directions

To compare homogeneity of forged and cast wheels material, velocities of shear waves were measured on slices cut from both wheel types. Ultrasonic waves were propagated in the z (hoop) direction and polarized in the x and y directions. Acoustic birefringence was calculated as a difference of t_y and t_z. Figure 9 shows the results of birefringence measurements along the line crossing the rim from FRF to BRF. For the forged wheel, texture-induced anisotropy is practically constant across the rim width. For cast wheels, rim structure is reflected, showing different values close to rim faces than in the inner region. A non-zero, positive B^0 value in the small, randomly oriented grain region, confirms data presented in Fig. 3 showing material anisotropy in this part of the rim.

Fig. 8 Examples of B^0 radial distribution in cast wheel stress relieved rim blocks

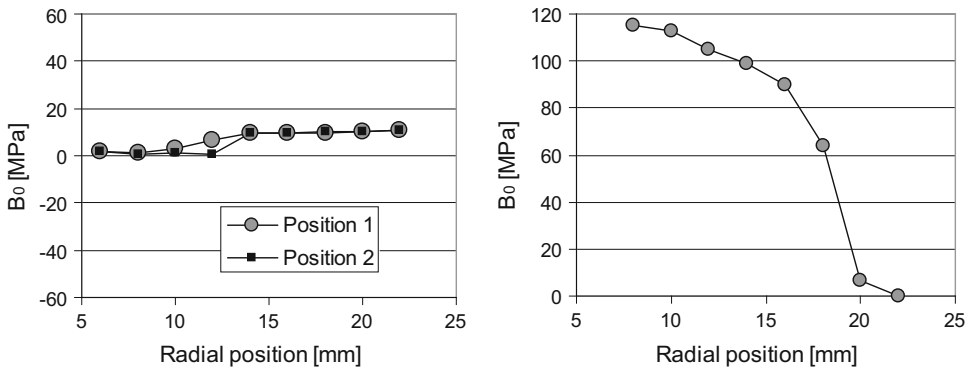

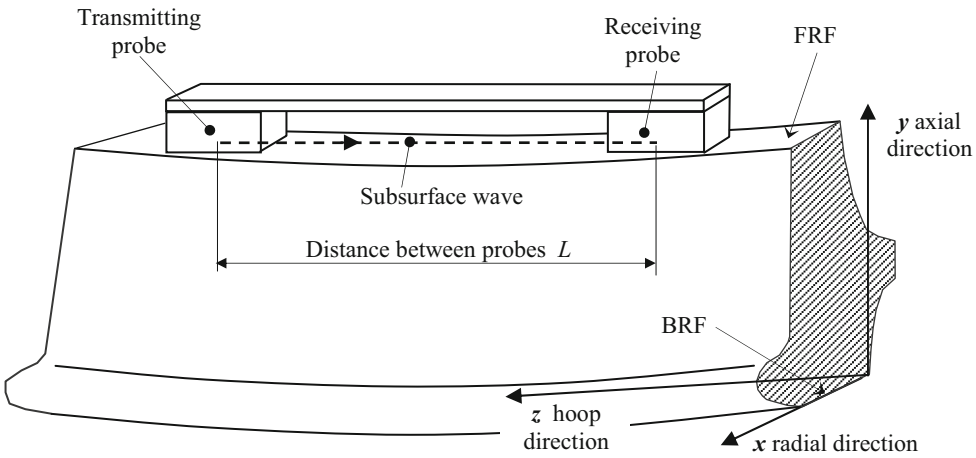

Fig. 10 Schema of hoop stress evaluation with subsurface wave in a monoblock wheel rim

3 Subsurface Waves

Residual stress evaluation with longitudinal subsurface waves was developed initially to evaluate the longitudinal component of residual stresses in railroad rails straightened with a roller straightener [37,38]. Longitudinal waves used in this technique are the most "stress sensitive" waves. When propagated along the stress, the elastoacoustic coefficient for this wave in steel is equal to $\beta_{111} = -1.25 \times 10^{-5}$ MPa^{-1} (compare this to elastoacoustic constants for acoustic birefringence equal to $\beta_B = -0.79 \times 10^{-5}$ MPa^{-1}). In railroad wheels, TOF of subsurface wave propagating in hoop direction can be measured on both FRF and BRF, according to Fig. 10.

The TOF of a longitudinal subsurface pulse measured between transmitting and receiving probes, in a stress-free rim, depends on the distance between probes, the velocity of the wave and temperature. Due to a slight texture gradient in the radial direction, observed in forged wheels, it depends also on radial position of the set of probeheads on rim face.

The TOF change due to stress, assuming constant distance between probes and constant temperature, is equal to:

$$t_L^\sigma - t_L^0 = t_L \left(\sigma_Z \beta_{ZZZ} + \sigma_X \beta_{ZZX} + \sigma_Y \beta_{ZZY}\right) \qquad (4)$$

where:

t_L^σ	TOF in stressed state,
t_L^0	TOF in stress free state (reference TOF),
$\sigma_X, \sigma_Y, \sigma_Z$	stress components,
β_{ijk}	elastoacoustic constants, indexes denote : i direction of wave propagation, j direction of wave polarization, k direction of stress.

On the rim faces $\sigma_Y$is zero. The value of β_{ZZX} describing the sensitivity of the longitudinal wave to stress component perpendicular to the wave propagation direction is small compared to β_{ZZZ}. Also, σ_X is small compared to σ_Z, and the influence of radial stress on measured TOF can be neglected. Value of hoop stress can be calculated as:

$$\sigma_Z = \frac{t_L^0 - t_L^\sigma}{t_L^\sigma \beta_{ZZZ}} \qquad (5)$$

The value of the elastoacoustic constant β_{ZZZ} was measured on samples cut of cast and rolled wheels and subjected to tensile tests. In [31] presented was $\beta_{ZZZ} = -1.47 \times 10^{-5}$ MPa^{-1} for cast wheels and in [12] $\beta_{ZZZ} = -1.25 \times 10^{-5}$ MPa^{-1} for European R7 steel forged wheels.

Measurement with subsurface waves provides stress values averaged in the thin, surface material layer between probeheads. This technique should provide stress values similar to resistance strain gauges or X-ray diffraction technique, both of which collect surface data.

Evaluations of hoop stresses in wheels using subsurface waves, described in [12,13,15,16,25,32], were performed with special, multitransducer sets of ultrasonic probes minimizing the influence of surface roughness on readings and equipped with temperature sensor for automatic temperature correction [39]. For this set of probes the distance on which TOF was measured was $L = 180$ mm. This distance is about the maximum probeheads spacing on rim faces, especially on narrow FRFs.

The use of subsurface waves on wheels allows to determine two values of hoop stress in the rim, on both rim faces, which helps to evaluated the stress gradient across the rim width. Extreme stress is often observed on one of these faces and maximum stress values determine if the wheel is considered safe or not.

According to formula 5, to calculate stress values, the reference TOFs t_L^0 have to be known. In general, if readings are to be taken on wheels made of various steel grades, on both FRF and BRF faces and for various radial positions on the rim face, numerous reference FOTs should be measured on

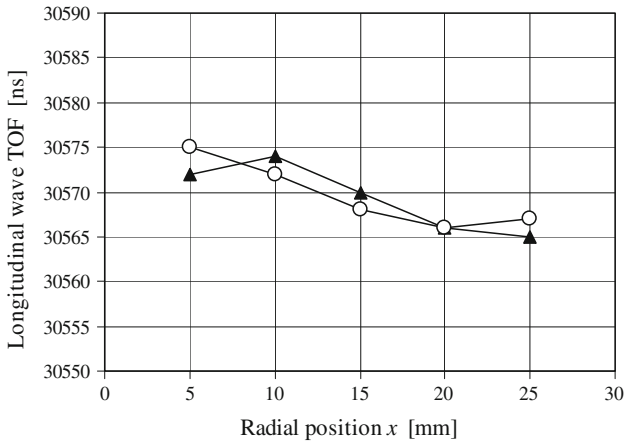

Fig. 11 Radial distribution of subsurface longitudinal TOF measured on BRF between casting risers (*white circles*) and close to carting risers (*black triangles*)

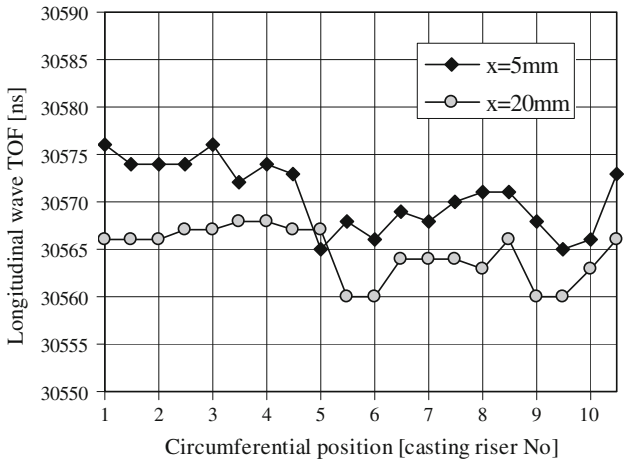

Fig. 12 Longitudinal subsurface TOF measured on front face of cast wheel for two radial positions of the probe head

numerous stress free blocks. The need to use numerous TOFs for device calibration is a weak point of using the subsurface wave technique for forged railroad wheels evaluation.

However, structure of a cast wheel gives an advantage to this technique. In such a wheel, texture on both rim faces is roughly identical and subsurface waves propagate along dendrites oriented normal to the surface. As a result, reference TOFs measured for longitudinal waves on both rim faces, for any radial position, are about the same. Figures 11 and 12 show radial and circumferential distribution of subsurface longitudinal waves on as manufactured cast wheel rim face.

Data presented on Figs. 11 and 12 confirm results of longitudinal wave velocity measurements performed with longitudinal wave on a small, rectangular sample cut from a cast wheel BRF. The velocity of longitudinal waves propagating in the z direction, in a columnar dendritic structure, is equal to 5918 m/s.

The scatter of TOFs measured for various radial positions of probeset on the rim face is equal to ± 5 ns. For a given radial position x, scatter over the wheel circumference in as-manufactured wheels, is equal to ± 8 ns. For the set of probeheads used in the measurements ($L = 181$ mm), this TOF difference corresponds to a stress difference equal to about ± 20 MPa. This leads to the conclusion that hoop stress in cast wheel can be evaluated using longitudinal subsurface waves, with acceptable precision, using only one reference TOF necessary to calibrate the device.

4 Stress Evaluation in Cast and Forged Wheels—Comparison

This chapter presents differences between stress development in cast and forged wheels subjected to braking in various conditions and measured with two described above ultrasonic techniques.

4.1 Rolled-Forged Wheels

Figure 13 shows readings taken on forged wheel subjected to several brakings, from 20 to 50 kW, in a test stand with the braking block centered on the tread. Acoustic birefringence and subsurface waves were measured in three locations, spaced 120° apart on the FRF [12]. White symbols present readings obtained with birefringence technique, black symbols show readings made using subsurface waves propagated along the FRF. It can be seen that brakings result in evenly distributed stress in the rim. Significant difference between rim width averaged stress (RWA) and surface stresses, equal to about 50 MPa, can be noticed for high power brakings numbered 17–22. For brakings up to No 17, the difference

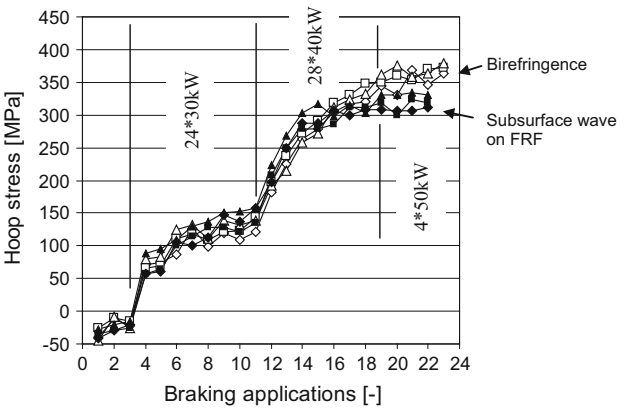

Fig. 13 Hoop stress development in forged wheel subjected to braking in stand, evaluated with acoustic birefringence technique and with subsurface longitudinal waves

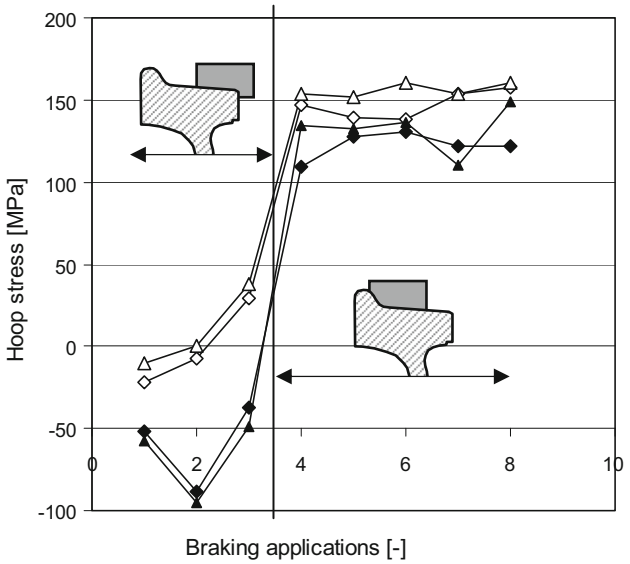

Fig. 14 Hoop stress development in forged wheel subjected to braking on track, evaluated with acoustic birefringence technique and with subsurface longitudinal waves

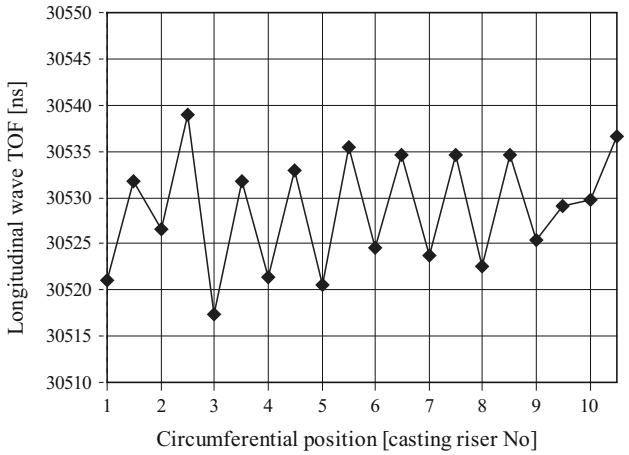

Fig. 15 Longitudinal subsurface wave TOFs measured on circumference of cast wheel subjected to 1 h, 80 hp braking in the dynamometer

between stress values evaluated with various techniques, in various positions on the rim, is below 50 MPa.

Figure 14 presents similar measurements, performed with the same equipment but in field conditions on forged wheel braked on track [12]. During the experiment, the brake block position was changed from overhanging (brakings No 1–3) to overriding (brakings No 4–8). Readings taken with acoustic birefringence (white symbols) and subsurface wave (black symbols) on the FRF differ significantly as reflected in stress distribution in the rim. Of interest is the first 20 kW of braking with overhanging brake block, resulting in the development of compressive stress on the FRF.

In forged wheels, with the exception of braking with overhanging brake blocks (see Fig. 14), no significant stress gradient was observed. It was also found that stress values measured at various points on the wheel circumference were in practice the same.

4.2 Cast Wheels

For some cast wheels subjected to braking in the dynamometer, it was noticed that ultrasonic readings taken with birefringence and subsurface waves differ depending on circumferential position of measurement, primarily between casting risers or close to them. Figure 15 shows, as a distinct example of such phenomena, results of subsurface longitudinal wave TOF readings taken on FRF of cast wheel after braking (59 kW, 1 h) [40]. Compared to circumferential readings taken on an as-manufactured cast wheel of the same type (Fig. 12) one can observe that the TOF pattern is different and related to the positions of casting risers. Longitudinal wave TOFs measured on FRF close to risers are lower by about 12 ns, corresponding to stress differences more than 30 MPa. What is more important, the average TOF in an as-manufactured wheel is higher by about 40 ns compared to wheels after braking, denoting development of a compressive hoop stress in the FRF surface layer.

Wheels described in [32,40] were cast, curved plate, class C wheels. For this particular wheel design, the plate is formed as a cone and the hub is shifted in axial direction with respect to the rim. Such a plate shape makes the wheel more resistance to hoop stress development due to thermal input but results also in significant stress gradient after severe brakings.

Measurements of hoop stress performed with birefringence and subsurface waves on several wheels of this design subjected to inductive heating [32] and braking in the dynamometer [40] showed that stresses on the wheel faces and averaged over the rim width differ significantly.

Figures 16 and 17 present the development of hoop surface stress on both rim faces and RWA stress for wheels subjected to braking in the dynamometer. Figure 16 shows results of measurements for the brake block overriding the wheel flang and in Fig. 17 for a brake block centered on the wheel tread. For the centered block position, braking powers was 60, 63, 67 and 75 kW. For the overriding block, the braking powers were 56, 60, 63 and 67 kW. It can be seen that regardless of brake block position, thermal loads due to braking resulted in the development of tensile stress on the BRF and RWA. On FRF compressive stress is developed.

The result of this stress gradient is relatively low increase on tensile RWA stress measured with acoustic birefringence technique. For the centered position of brake blocks, RWA stress increased by about 60 MPa. For overriding brake positions, this was only about 20 MPa. As mentioned earlier high scatter of texture induced anisotropy B° was observed in cast

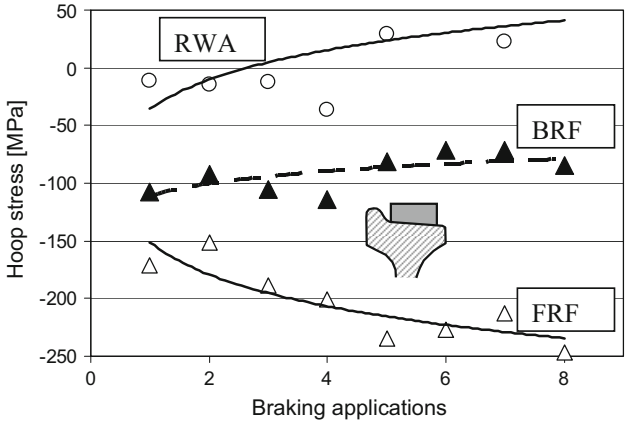

Fig. 16 Hoop stress development in cast curved plate, class C wheels due to braking in a dynamometer. Results for braking with brake block centered

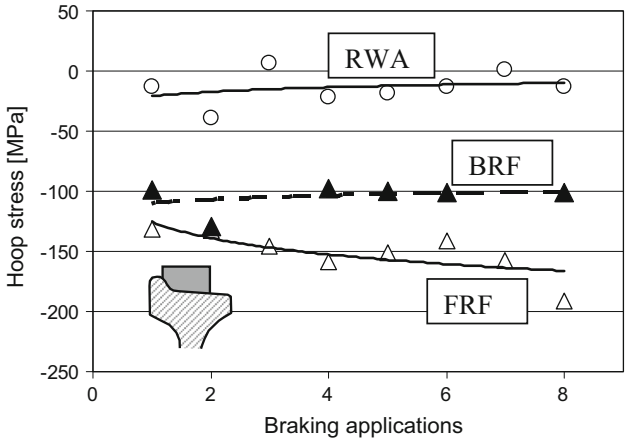

Fig. 17 Hoop stress development in cast curved plate, class C wheels due to braking in a dynamometer. Results for braking with braking block flanged

wheels currently tested. This scatter, reported as ±80 MPa in [35] and as ±40 MPa in [32], is of the same order as RWA stress changes due to several high power braking applications. Therefore, without a significant improvement in determination of B° in cast wheels, the ultrasonic technique based on acoustic birefringence measurement seems to be limited, able to identify only extremely overheated wheels of this design.

The measure of stress gradients in the wheel rim is the difference between stresses on both rim faces, compressive on FRF and tensile on BRF.

Figures 16 and 17 show that surface stress on FRF changes in course of braking with the brake block centered and overriding the flange by about −80 and −40 MPa, respectively. The same stress changes observed on BRF are lower and equal to about 30 and 15 MPa, respectively. Evaluation of stress differences between FRF and BRF seem to be a practical measure of stress states in wheels of this type. For as-manufactured wheels, surface stress differences are only about 30 MPa. After final braking, this difference is about 120 MPa for overriding brake blocks and about 150 MPa for centered brake blocks. These stress changes are much higher than those measured with RWA stress increase.

The acoustic birefringence method, which averages data over a relatively small volume of material, is sensitive to any variation of rim material texture. The subsurface wave technique averages data over a distance of about 150–200 mm, depending on probehead design, making this technique less sensitive to texture changes connected with casting riser positions.

Figures 11 and 12 demonstrate that in cast wheels, surface stress can be evaluated with longitudinal subsurface wave, without any texture correction, thanks to repeatable material structure on wheel surfaces. Figures 16 and 17 show that without any calibration (without reference TOF measurements on a stress free rim block) the comparison of longitudinal wave TOFs on both rim faces is a measure of stress state in the rim.

5 Conclusions

Despite the same mechanism of dangerous hoop stress development in forged and cast wheels, these two types of monoblock wheels present different problems for ultrasonic stress evaluation. Modern European forged wheels demonstrate low and uniform over the circumference texture-induced acoustic anisotropy. Thermal loads during braking result in stresses evenly distributed on the wheel circumference, with a stress gradient in the radial (x) direction. In general values of stress measured on the rim faces are approximately the same as stress averaged over the rim width. The evaluation of hoop stresses using the acoustic birefringence technique provides reliable information concerning the stress state in the forged wheel rim. Thanks to uniform circumferential stress distributions, measurements of acoustic birefringence can be limited to few test positions only.

The structure of cast wheels makes ultrasonic stress evaluation in these wheels more difficult. Cast wheels present complex structure both in the rim cross section and along the rim circumference. The value of texture-induced acoustic anisotropy is higher compared to forged wheels, and data presented in the literature show its high scatter. Data concerning an elastoacoustic coefficient for cast wheels are limited and also present significant scatter. Experiments in laboratory conditions showed that hoop stress developed during braking or inductive heating in cast wheels is irregular probably due to the influence of casting risers. In some cast wheels, positions of the casting risers are unknown. Therefore, to evaluate stress states in such wheels, several readings should be taken on the wheel circumference and a mean stress value calculated.

Averaged stress evaluated using the acoustic birefringence in cast, curved plate wheels is a weak measure of stress state due to significant stress gradient in axial (y) direction. The most promising and practical technique to evaluate stress states in curved plate wheels seems to be measurement of longitudinal wave TOF on both rim faces. The structure of cast wheel is advantageous in such measurements. On both rim faces, longitudinal wave propagates perpendicular to dendrites that are oriented normal to the surface. The velocity of longitudinal waves for a specific stress free wheel should be the same on both its faces. Therefore, the measurement of the difference front-back rim face stress can be performed without any calibration or reference TOF determination and should deliver data concerning stress sate in the rim.

References

1. Johnson, M.R., Robinson, R.R., Opinsky, A.J., Detone, D.H.: Railroad Wheel Back Rim Face Failures: III—Residual Stress Calculations on 33" D One-Wear Freight Car Wheels. Association of American Railroads, Technical Center Report No. R-560, Chicago (1983)
2. Kuhlman, C., Gallagher, M.: The significance of material properties on stress developed during quenching of railroad wheels. In: Hawthorne, V. T., Kneschke, T. (eds.) Proceedings of Joint ASME/IEEE Railroad Conference, Book No. 100265, pp. 55–63 (1988)
3. Barton, J.R., Perry, W.D., Swanson, R.K., Hsu, G.C., Ditmeyer, S.R.: Heat-discolored wheels: safe to refuse? Prog. Railroad. **28**(3), 841–848 (1985)
4. Utrata, D., Namkung, M.: Assessment of the magnetoacousic method for residual stress detection in railroad wheels. Rev. Prog. Q. **12B**, 1807–1814 (1993)
5. Langman, R.A., Muton, P.J.: Estimation of residual stresses in railway wheels by means of stress-induced magnetic anisotropy. NDT&E Int. **26**, 195–205 (1993)
6. Nishimura, S., Tokimasa, K.: Study on the residual stresses in railroad solid wheels and their effect on wheel fracture. Bull. JSME **18**, 459–468 (1976)
7. Iwand, H.C.: A comparative analysis using Barkhausen noise analysis, ultrasonic birefringence and saw cutting techniques in determination of residual stress in railroad Wheel. University of Nebraska, Thesis (1988)
8. Benson RW (1968) Development of nondestructive methods for determining residual stress and fatigue damage in metals, NASA Marshall Space Flight Report, Contract No. NAS8-20208.
9. Fukuoka, H., Toda, H., Hirakawa, K., Sakamoto, H., Yoya, Y.: Acoustoelastic measurements of residua stresses in the rim of railroad wheels. Wave Propag. Inhomog. Media Ultrason. Nondestr. Eval. **6**, 185–193 (1984)
10. Clark Jr, A.V., Fukuoka, H., Mitrakovic, D.V., Moulder, J.C.: Characterization of residual stress and texture in cast steel railroad wheels. Ultrasonic **24**, 281–8 (1986)
11. Clark, A.V., Fukuoka, H., Mitrakovic, D.V., Moulder, J.C.: Ultrasonic characterization of residual stress and texture in cast steel railroad wheels. Rev. Prog. Q. **6B**, 1567–1575 (1987)
12. Draft Control Committee Office for research and Experiments of the International Union of Railways, Question B169: Thermal limits of wheels and shoes. Report No. 2. Effect of frequent braking on the residual stress field in the wheel rim. Utrecht, The Netherlands, April 1989.
13. Deputat, J., Osuch, K., Kunes, W.: Untesuchung der Eigenspannungsanderungen in Eisenbahn-Vollradrn nach Bremsungen. Glasers Annalen (J. Railw. Transp.) **115**, 231–235 (1991)
14. Schneider, E.: Ultrasonic birefringence effect—its application for materials characterizations. Opt. Laser Eng. **22**, 305–323 (1995)
15. ERRI/B169 Committee, Monitoring solid wheels in service. In: Proceedings 11th International Wheelsets Congress, Paris, vol. 1, pp. 149–54 (1995)
16. Osuch, K., Stone, D.H., Orringer, O.: European and American wheels and their resistance to thermal damage. In: Proceedings of 11th International Wheelsets Congress, Paris. vol. 1, pp. 77–86 (1995)
17. Stone, D., Garcia, G., Burnett, S.: An evaluation of residual stress in cast steel railroad wheels using electromagnetic acoustic transducers (EMATs) U.S. Department of Transportation, Federal Railroad Administration, Office of Research and Development Washington, D.C. 20590 Final Report (1998)
18. Institute of Fundamental Technological Research: DEBRO Ultrasonic Stress Meter. Polish Academy of Science, Warsaw (1990)
19. Bartosiewicz, A., Mizerski, K., Deputat, J., Szelążek, J.: Miniature ultrasonic stress gauge for in-service detection of thermally damaged wheels. In: Proceedings of 11th International Wheelsets Congress, Paris. vol. 19951, pp. 241–243 (1995)
20. Schneider, E., Herzer, R., Bruche, D., Frotscher, H.: Ultrasonic characterization of stress states in rims of railarod wheels. In: Green, R.E., et al. (eds.) Nondestructive Characterization of Materials VI, pp. 383–390. Plenum Press, New York (1994)
21. Schramm, R.E.: Ultrasonic measurement of stress In railroad Wheel. Rev. Sci. Instrum. **70**, 1468–1473 (1999)
22. Limal, J.L., Del Fabro, V.: Prevention of thermal damage in railroad wheels thanks to the monitoring of residual stresses by ultrasonic examination. In: Proceedings of 11th International Symposium Assessment of Materials Aiging and Damage Evolution by Non Destructive Evaluation methods, Cercle d'Etudes Des Metaux, St. Etienne, TOME XVI Chapter 17 (1995)
23. European Committee for Standardization, Railway applications—Wheelsets and bogies— Wheels: Product requirements. European Standard CEN 13262 (2004)
24. Lonsdale, C., Bogacz, R., Norton, M.: Application of pressure poured cast wheel technology for European freight service, Proceedings of 9th World Congress on Railway research, May 22–26, Lille, France, Chalenge C: Increasing freight capacity and services (2011)
25. CNTK: Final Report, Joint Research project MT/DOT-92-115, Investigation of wheels thermal damage mechanism and elaboration of method for wheel failure prevention, CNTK, Warsaw (1996)
26. Cookson, J.M., Muton, P.J., Lynch, M.R.: Validation, Calibration and application of ultrasonic residual stress measurement systems to railway wheels. In: Proceedings 15th International Wheelset Congtress, Prague, September 23–27 (2007)
27. Del Fabro, V., Catot, B.: Ultrasonic measurement of stresses in new wheels. In: Proceedings of 11th International Wheelset Congress, Paris, pp. 251–299 (1995).
28. Kamyshev, A.V., Nikitina, N.E., Smirnov, V.A.: Measurement of the residual stresses in the treads of railway wheels by the acoustoelasticity method. Russ. J. Nondestruct. **46**, 189–193 (2010)
29. Dymkin, GYa., Krasnobryzhii, S.A., Shevelev, A.V.: An ultrasonic method for measuring residual mechanical stresses in the rims of solid-rolled railroad wheels that considers the intrinsic anisotropy of the material. Russ. J. Nondestruct. **49**, 8–14 (2013)
30. Okada, K.: Stress-acoustic relations for stress measurement by ultrasonic technique. J. Acoust. Soc. Jpn. **1**, 193–200 (1980)
31. Deputat, J.: Effect of braking application on residual stress in the rim of railroad wheels. In: Proceedings Conference on Roling Noise

Generation, Technische Universitaet, Berlin, Germany pp. 159–68 (1989)
32. Schramm, R.E., Szelążek, J., Clark, A.V.: Residual stress in induction-heated railroad wheels: ultrasonic and saw cut measurements, NISTIR 5038, Report No. 28. National Institute of Standards and technology, Boulder (1995)
33. Ultrasonic method for determining the residua stress in the rim (nondestructive method), Standard EN 13262:2004, Annex D.
34. Schneider, E., Herzer, R.: Ultrasonic Evaluation of Stresses in the Rims of Railroad Wheels. In: Proceedings of 7th ECNDT Copenhagen, May 26–29. vol. 2, pp. 1972–1979 (1998)
35. Schramm, R.E., Clark, A.V., Mitrakowic, D.V., Schaps, S.R., McGuire, T.J.: Residual stress detection in railroad wheels: an ultrasonic system using EMATs. NISTIR 3968, Report No. 23, National Institute of Standards and Technology, Boulder (1991)
36. Szelążek, J.: Ultrasonic stress evaluation in cast railroad wheels. Arch. Foundry **6**, 509–524 (2006). (in Polish)
37. Egle, D.M., Bray, D.E.: Measurement of acoustielasticity and third order elastic constants for rail steel. J. Acoust. Soc. Am. **60**, 741–744 (1976)
38. Brokowski, A., Deputat, J.: Ultrasonic measurements of residua stress in rails. In: Proceedings of 11th World Conference on Nondestructive testing, Columbus, vol. 1, pp. 592–598 (1985)
39. Szelążek, J.: Sets of piezoelectric probeheads for stress evaluation with subsurface waves. J. Nondestruct. Eval. **3**(32), 188–199 (2013)
40. Schramm, R.E., Szelążek, J., Clark, A.V.: Dynamometer-induced Residual Stress in Railroad Wheels: Ultrasonic and Saw Cut Measurements. NISTIR 5043, Report No. 30, National Institute of Standards and Technology, Boulder (1995)